

Investigating the Effect of Sudden Stratospheric Warming on the Ionosphere above Basrah City

Hawraa Hazim and Najat M. R. Al-Ubaidi^{1b*}

¹Department of Astronomy and Space, College of Science, University of Baghdad, Baghdad, Iraq

^{b*}Corresponding author: najat.raoof@sc.uobaghdad.edu.iq

Abstract

The sudden thermal warming phenomenon in the stratosphere (SSW) occurred during wintertime, an important thing affecting communication throughout the ionosphere region. This study looks at how the SSW through the stratosphere temperature peak affects the three ionosphere parameters: the total electron content (TEC), the critical frequency foE, and the foF2 of two layers, E and F2. It uses the IRI-20 model over Basrah city, which is in the south of Iraq and lies at 30.4°N 47.7°E. This study spans 2014 and 2019, during the 24th solar cycle. In the same years, 10 hPa pressure heights are taken for hourly stratosphere temperature. It was found that there are (7) SSW events during the period selected, three in 2014 and four in 2019. The relation between stratospheric temperatures and ionospheric parameters was studied to find this effect. The results revealed non-linear relations between them during all event hours, but there is an increase in ionization. The TEC variation is remarkably present in all events, with positive ionization enhancement during the daytime, reaching a maximum in the afternoon and then going down after the sun sets. The foE and foF2 measurements also show a small change due to changes in the thermosphere's make-up, temperature, winds, and either the F region dynamo or the E region dynamo. These changes also have an impact on the TEC enhancement values. This increment in values for the ionospheric parameters is irregular with time and varies from one parameter to another.

Article Info.

Keywords:

Basrah City, Critical Frequency, Ionosphere, SSW, TEC.

Article history:

Received: Sep.04, 2024

Revised: Dec. 07, 2024

Accepted: Dec. 24, 2024

Published: Mar. 01, 2025

1. Introduction

The layer of Earth's atmosphere that affect Earth's ionosphere is called stratosphere, this layer is within the pressure height level of 10hpa (~30km) above Earth's surface. This layer is very important through its effect on the electron density of the ionosphere layers [1]. The Earth's stratosphere is the conversion area, which communicates with both the ionized upper region in the high atmosphere (the Earth's ionosphere, which is very important in communications or radio wave propagation) and the lower atmosphere (troposphere) [2, 3]. Consequently, the thermal structure, energy composition, dynamics, chemistry, and functions in controlling high-frequency radio propagation on Earth present difficulties for communications researchers in this area of the atmosphere [4, 5]. The impact of the rapid variations in temperature and zonal circulation in the polar stratosphere extends vertically up towards the mesosphere, where the ionosphere is found [6] and extends horizontally into low and mid-latitude regions. This revealed temperature rises in the stratosphere occurring in winter [7]. The event continues for a few days, while the warming sometimes lasts for weeks or month depending on the kind of event that was affected by the polar vortex strength [8]. These temperature rises often occur at 10 hPa in the middle stratosphere. Tens of degrees Celsius of fast temperature rise persist for several days or weeks. A phenomenon known as sudden stratospheric warming (SSW) occurs when the westerly polar winds in the stratosphere are occasionally reversed and the polar vortex is shifted [9]. This phenomenon affects how the Earth's atmosphere circulates through the troposphere, mesosphere, and ionosphere. It also changes atmospheric pressure, winds, water vapor



distribution, and other factors [10-13]. During the chilly winter months, the zonal wind, which normally blows eastward, can occasionally shift or even reverse and move westward, changing how it interacts with planetary waves. Disturbances in the upward planetary wave and zonal wind interaction are linked to this meteorological occurrence [14]. Over several days, the polar stratospheric temperature rises as a result of this alteration in its interaction. An unexpected link between low, mid, and high latitudes at thermosphere and ionosphere altitudes during SSW episodes was recently discovered [15, 16].

Many studies made by Pedatella et al. during 2010 – 2018 examined the impacts of solar wave variability and atmospheric tides during SSWs on the ionosphere for low- and mid-latitude regions, as well as the influence of SSWs on the entire atmosphere and the relationship between the thermosphere, ionosphere, and mesosphere [17-21]. In 2022, Pedatella and Harvey investigated the circulation, atmospheric tides in the mesosphere and lower thermosphere, and the zonal mean temperature [22]. In 2023, Pedatella studied how SSW affected ionosphere plasma densities and electrodynamics during weak polar vortex states and how it affected thermosphere composition, temperature, and winds [23]. Other researchers from 2012-2022 focused on the worldwide reaction of the ionospheric and thermospheric layers to the major and minor SSW events [24-29]. Others focused on the 2018 SSW event, such as Wang et al. in 2019, studied the impact of the winter major SSW of 2018 on the mid-latitude mesosphere at (70–85) km altitudes [30]. Liu et al. studied the ionospheric reaction to the abrupt stratospheric warming event of 2018 in middle- and low-latitude sites over China [31]. Shi et al., in 2024, discovered that both downward and to the lowest stratosphere did the positive stratospheric temperature anomaly travel and equator-ward reaching mid-latitudes of Eastern Europe and Asia through the impact of 2018 SSW [32]. Greer et al., in 2023, examined the polar vortex strength in mid-latitude and in different longitudes on the composition of the thermosphere and ionospheric plasma density in the Asian sector [33]; in the same year, Jinee et al. examined the significant and minor SSW occurrences that took place throughout the time in the Northern Hemisphere (1981–2020) [34]. As a result, it is critical to track, examine, and comprehend how SSW affects the ionosphere in mid-latitude areas of the Earth.

This study examines the relationship between the ionosphere and stratosphere, especially through the temperature peak variation at a pressure height of 10hpa and the ionosphere parameters for E and F2-layers and the Total Electron Content (TEC) above Basrah city in the South of Iraq located at mid-latitude region in the Northern hemisphere. Basrah City was chosen as a study case to investigate the effect of SSW events that occurred during 2014 and 2019 on the ionosphere through the ionization response.

2. Data and Methodology

2.1. Study Area

To understand the effect of SSW on the ionosphere above Basrah city/ Iraq, the studied area was geographically confined to four main areas: The western desert plateau located to the west of the Euphrates River, the northern Iraqi highlands, the southern coastal plain, and the region between the rivers Euphrates and Tigris. Some information should be known about this region, especially its location in the southwest of Asia and the northern hemisphere in the mid-latitude region [35, 36]. In this research, Basrah city (30.4°N; 47.7°E) was taken as a study case (shown in Fig. 1).



Figure 1: Iraq map with Basra city.

2.2. Data Selection

Data for hourly temperatures from the ERA5 satellite are downloaded at an altitude of 10hpa ($\sim 30\text{km}$) in the stratosphere. The fifth-generation ECMWF reanalysis provides a comprehensive dataset spanning over eight decades from 1940. This reanalysis merges model data with global observations through data assimilation, ensuring a consistent and complete dataset. The extraction process involves selecting specific parameters, such as time in coordinated universal time (UTC), geographical area (longitude and latitude), and data format to obtain relevant temperature data for the designated region, cited in (<https://cds.climate.copernicus.eu/cdsapp#!/dataset>).

The solar indices sunspot numbers (SSN) and flux $F_{10.7}$ in solar flux unit (sfu, $1 \text{ sfu} = 10^{-22} \text{ W m}^{-2} \text{ Hz}^{-1}$) were taken from Word Data Center (https://www.ukssdc.ac.uk/wdcc1/data_menu.html), while the disturbance storm time index (Dst) in (nT) unit based on the presence or absence of a geomagnetic storm was taken from the Kyoto Japan WDC, cited in (<http://wdc.kugi.kyoto-u.ac.jp/dst>) for the same selected period. The ionospheric parameters, critical frequency (in MHz) of E-layer (foE) and of F2-layer (foF2) and the total electron content ($\text{TEC} \times 10^{16}$ in electrons/ m^2) were calculated from the International Ionospheric Model (IRI-20) over Basrah city [37-40], the citation of this model (<https://irimodel.org/>).

2.3. Data Analysis

The years 2014 and 2019 were selected for this study. The criteria of this choosing were for maximum and minimum solar activity in these two years, respectively. To avoid any solar activity effect during the selected years, the solar indices sunspot numbers (SSN), Flux ($F_{10.7}$) and geomagnetic disturbance storm time index (Dst) were taken for the same period, as illustrated in Figs 2-4, respectively. From these figures, it was found that there are no geomagnetic storm effects. From the Dst

values, it appears that the Sun is in a quiet condition; also, the other indices, the spot number and solar flux radiation, are not high [31, 41].

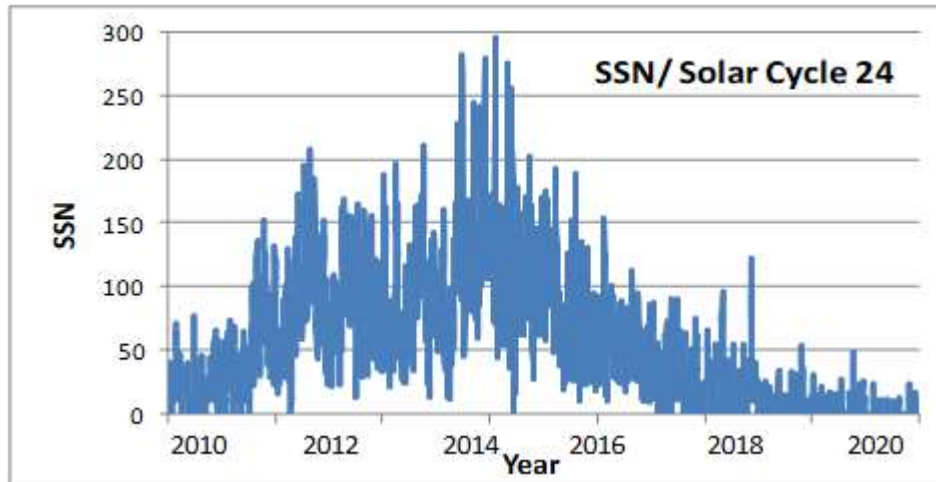


Figure 2: Daily SSN for Solar Cycle 24 [https://www.ukssdc.ac.uk/cgi-bin/wdccc1/secure/geophysical_data].

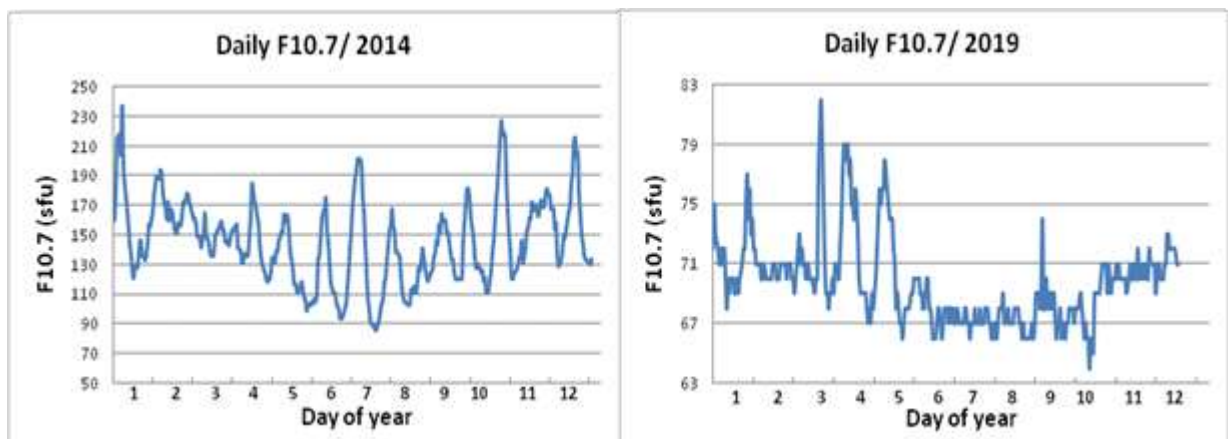


Figure 3: Daily F10.7 (sfu) during events of two years 2014 and 2015.

The hourly temperature data over Basrah city for these two years was taken at pressure height level of 10hpa (~30km) in the stratosphere, as shown in Fig. 5. From analyzing the temperature data, it was found that there were seven SSW events in these two years, three in 2014 and four in 2019 distributed as in Table 1.

To study the impacts of these seven events during the period selected on the Earth's ionosphere, three different ionospheric levels for three ionospheric parameters were chosen: the critical frequency (in MHz) for E-layer (foE) at 100km and for F2 layer (foF2) at 300km and TEC (in electrons/m²) at 500km. Figs. 6 - 12 reveal the hourly stratosphere temperature in Kelvin for the three ionospheric parameters (foE, foF2 and TEC) for the seven SSW events. Figs 6-8 illustrate events 1-3, respectively for 2014 in which the SSN was maximum and Figs 9-12 represent the events 4-7, respectively for 2019 in which the SSN was minimum from the solar cycle 24. It can be noted that the critical frequency (f_{cr}) (in MHz) is related to the electron density (N_e) (in electrons/m³) by the following Eq. 1 [42-44]:

$$f_{cr} = \sqrt{\frac{N_e}{1.24 \times 10^{10}}} \quad (1)$$

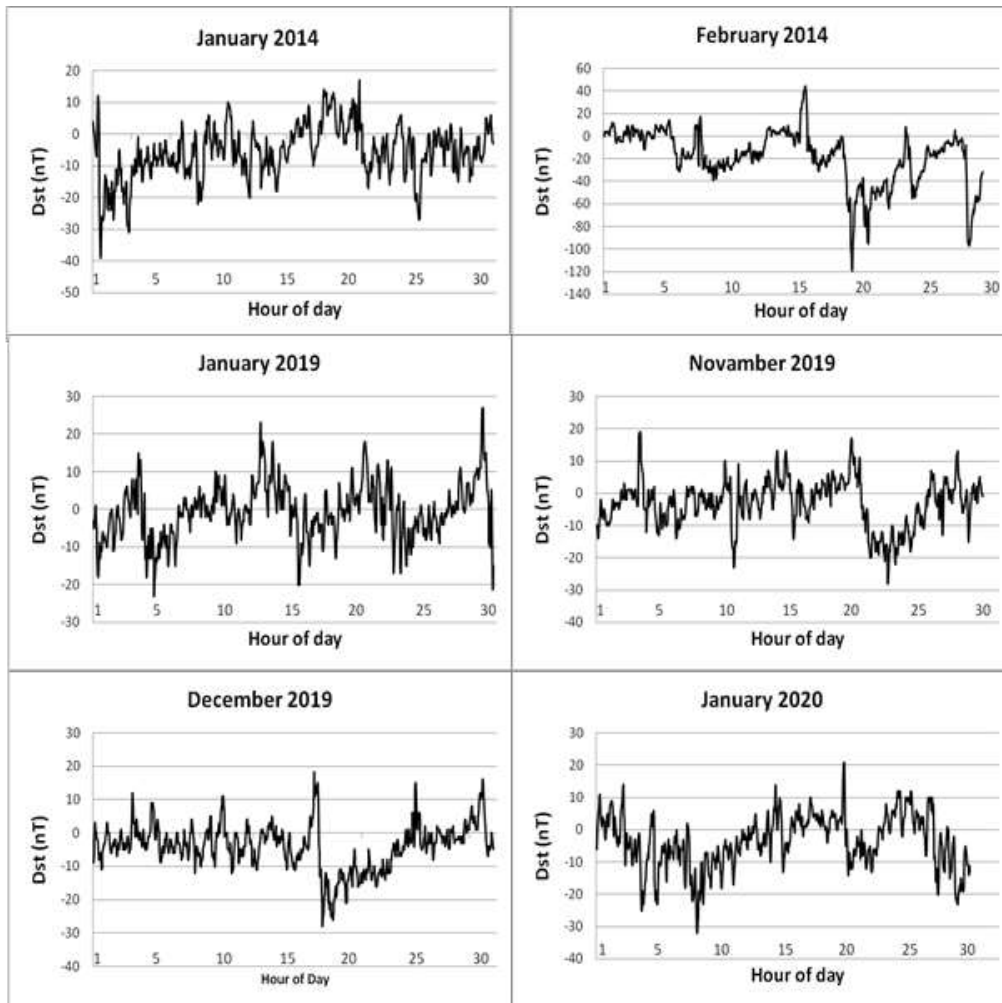


Figure 4: Hourly Dst (nT) during events of two years 2014 and 2019.

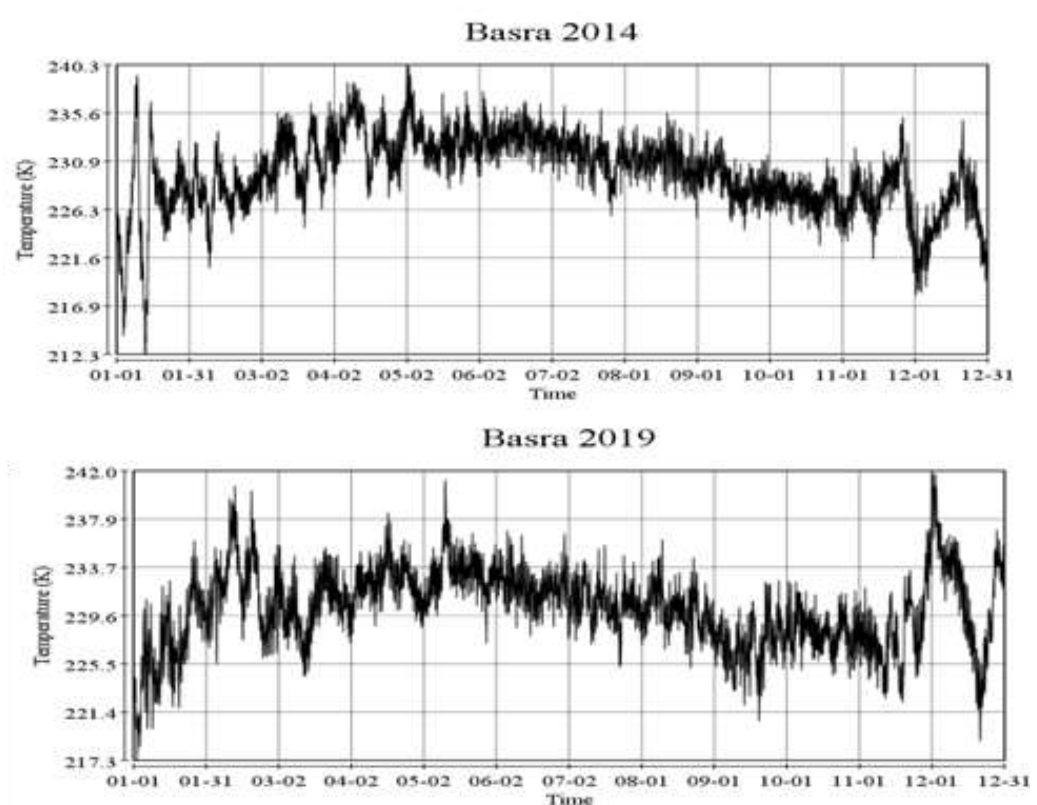


Figure 5: Temperature for Basrah above 10hpa during 2014 and 2019.

Table 1: SSW events for 2014 and 2019, their start and end dates with temperature, temperature maximum, duration time, and temperature difference between start and end.

Event No.	Year	Start date (dd.mm.hh)	T (K)	Max date (dd.mm.hh)	T _{Max} (K)	ΔT (K)	End date (dd.mm.hh)	T (K)	Duration (hour)	Increase temperature percentage
1	2014	3-1-9 pm	214	9-1-1 pm	239.2	25.2	12-1-8 pm	212.9	216	11.7757
2	2014	12-1-9 pm	212.3	15-1-9 am	236.7	24.4	17-1-6 am	226.8	106	10.91846
3	2014	8-2-8 pm	220.6	12-2-9 am	233.8	13.2	14-2-8 am	227.3	133	5.98368
4	2019	2-1-4 pm	217.9	6-1-11 am	231	13.1	8-1-11 pm	219.9	152	6.0119
5	2019	19-11-6 am	222.2	22-11-9 am	233.5	11.3	25-11-1 am	224.7	140	5.0855
6	2019	26-11-5 pm	225.5	1-12-11 am	242	16.5	21-12-5 pm	218.9	601	7.3171
7	2019-2020	21-12-5 pm	218.9	28-12-6 pm	236.9	18	10-1-9 pm	220.7	484	8.2229

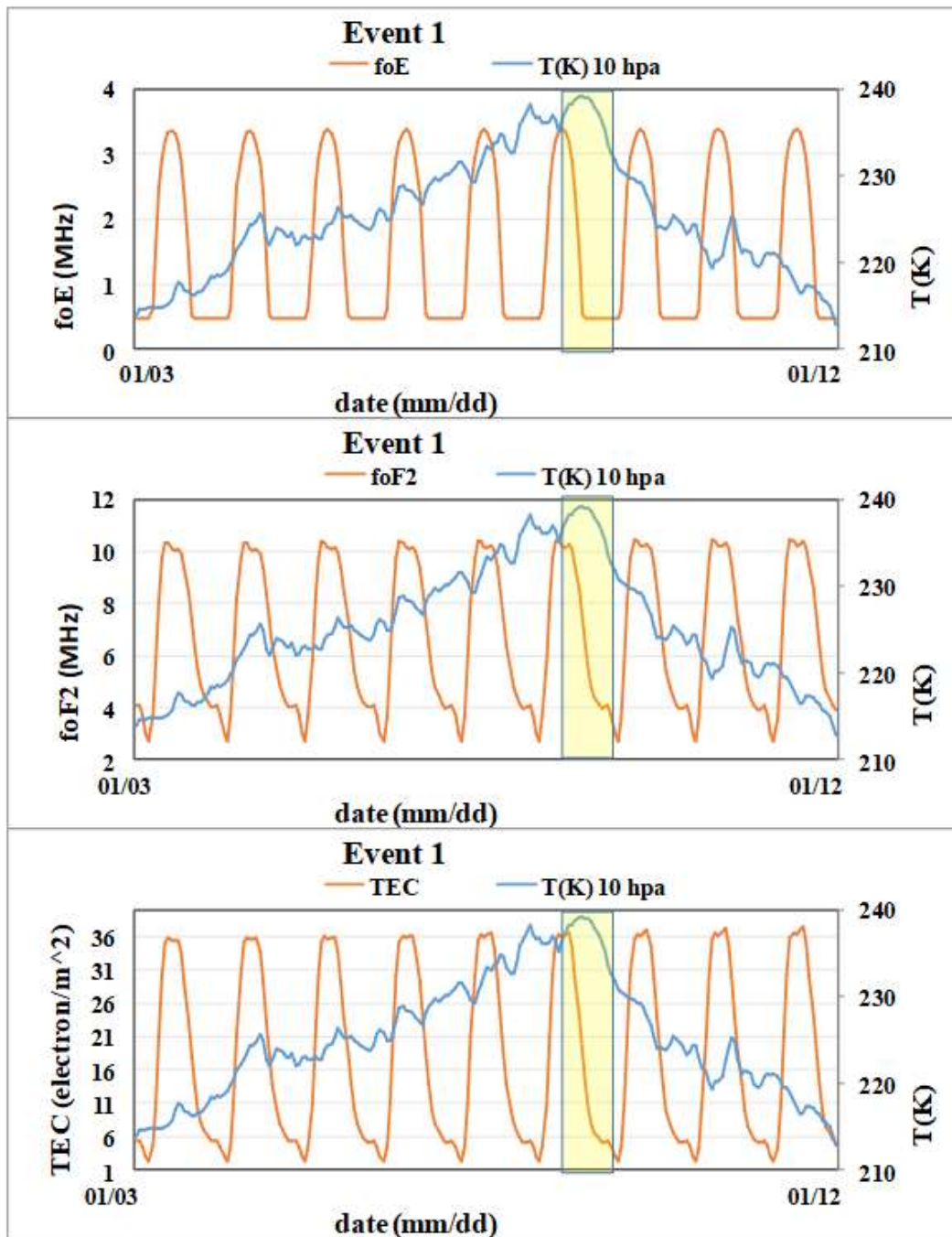


Figure 6: Ionospheric parameters with stratosphere temperature for event 1 year 2014.

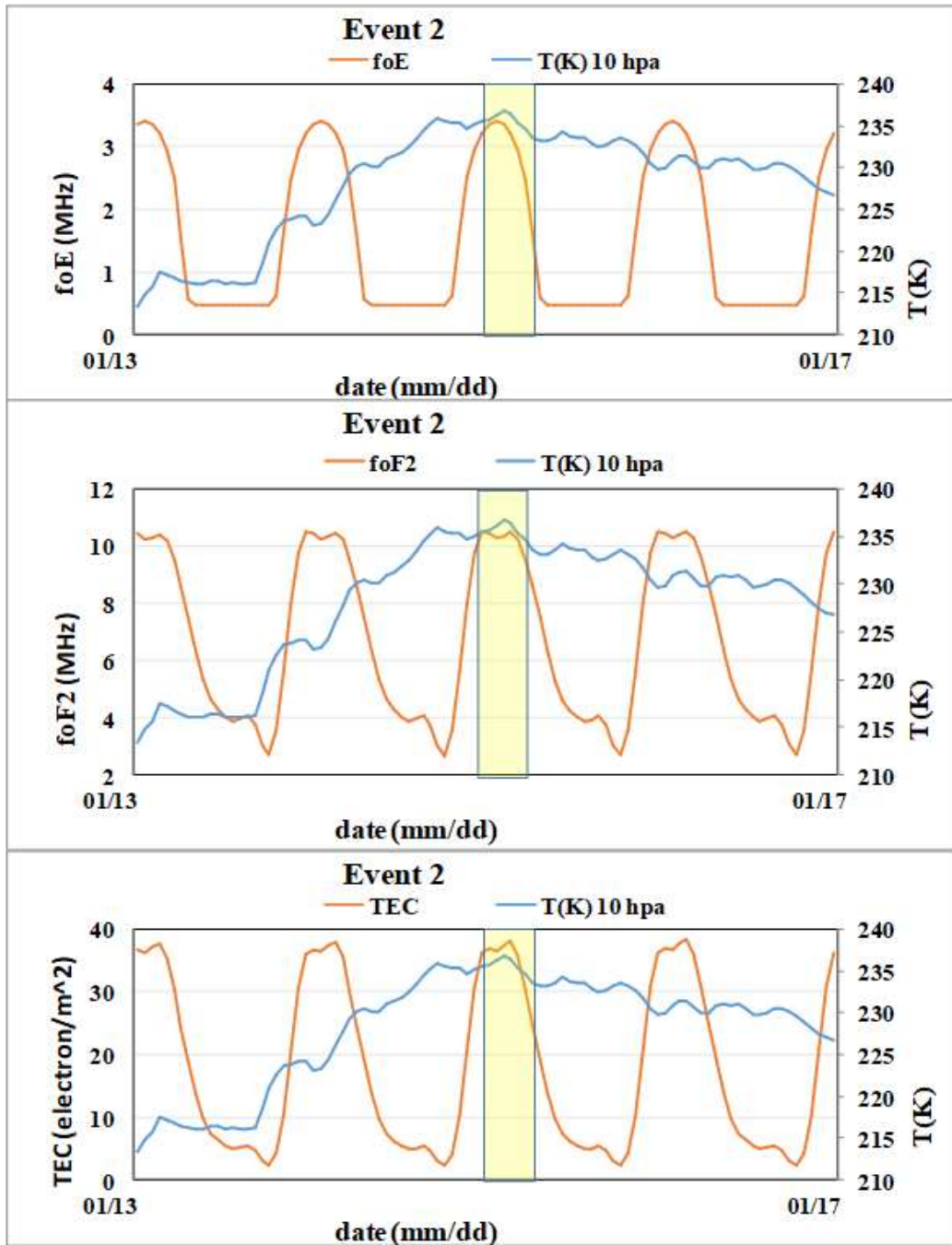


Figure 7: Ionospheric parameters with stratosphere temperature for event 2 year 2014.

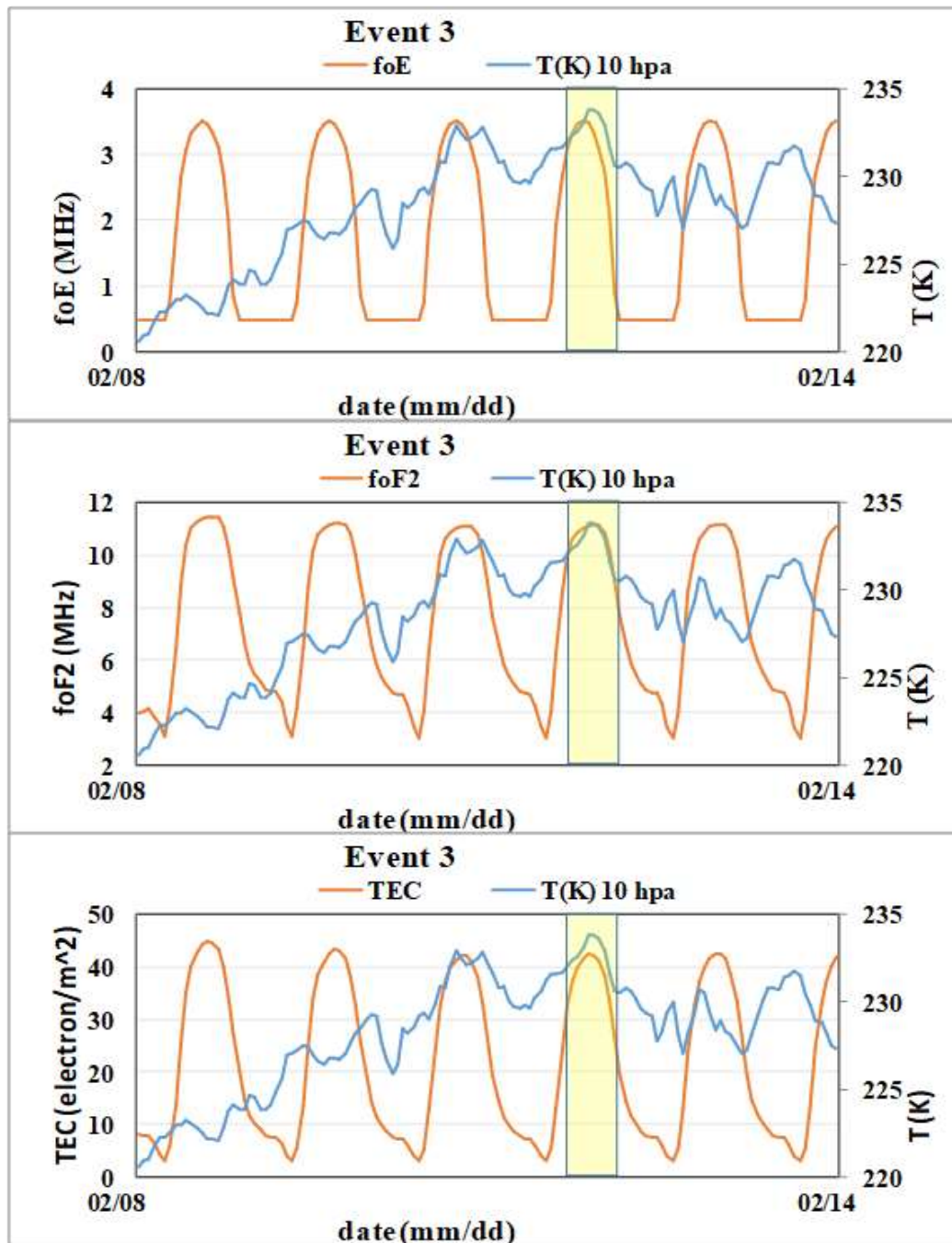


Figure 8: Ionospheric parameters with stratosphere temperature for event 3 year 2014.

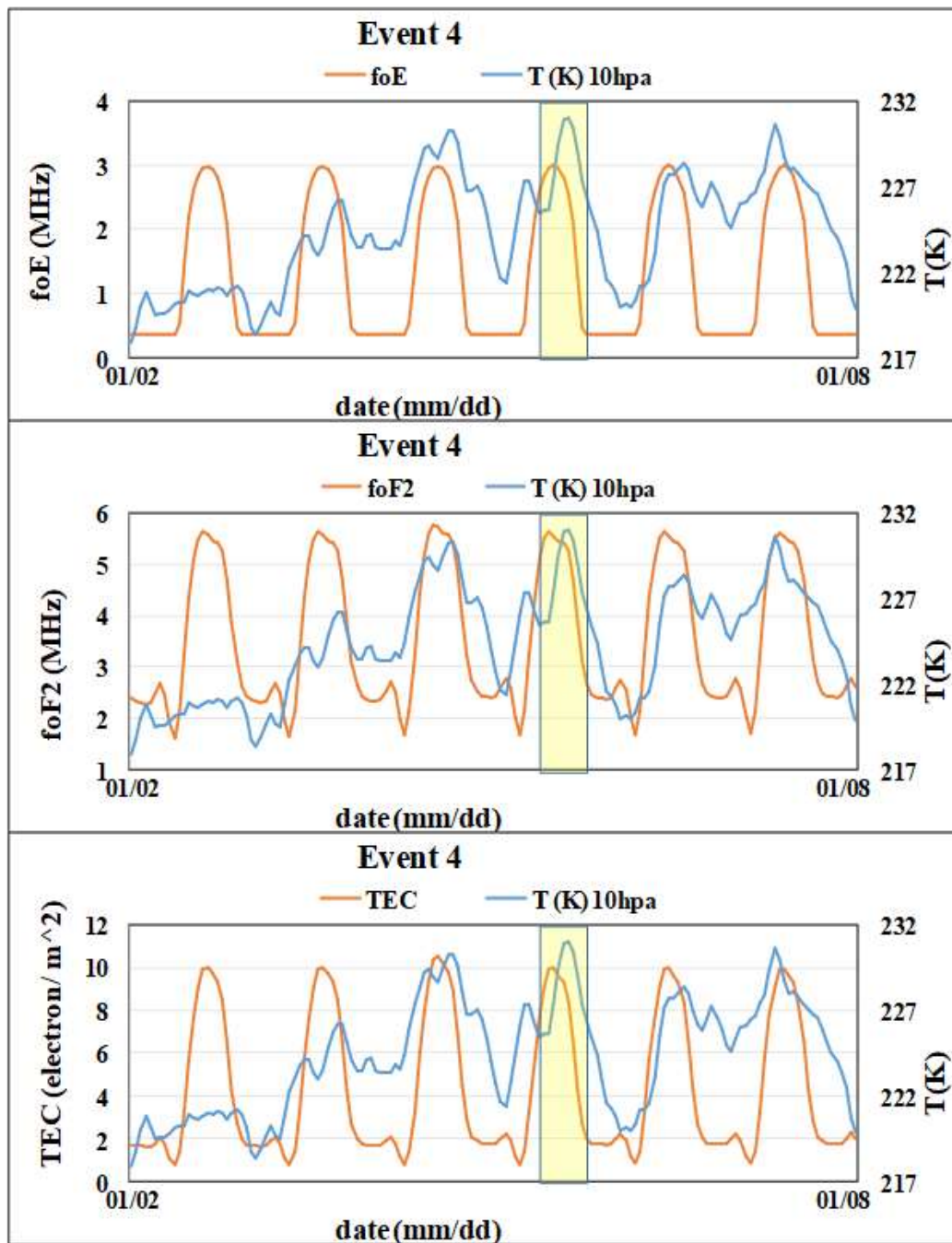


Figure 9: Ionospheric parameters with stratosphere temperature for event 4 year 2019.

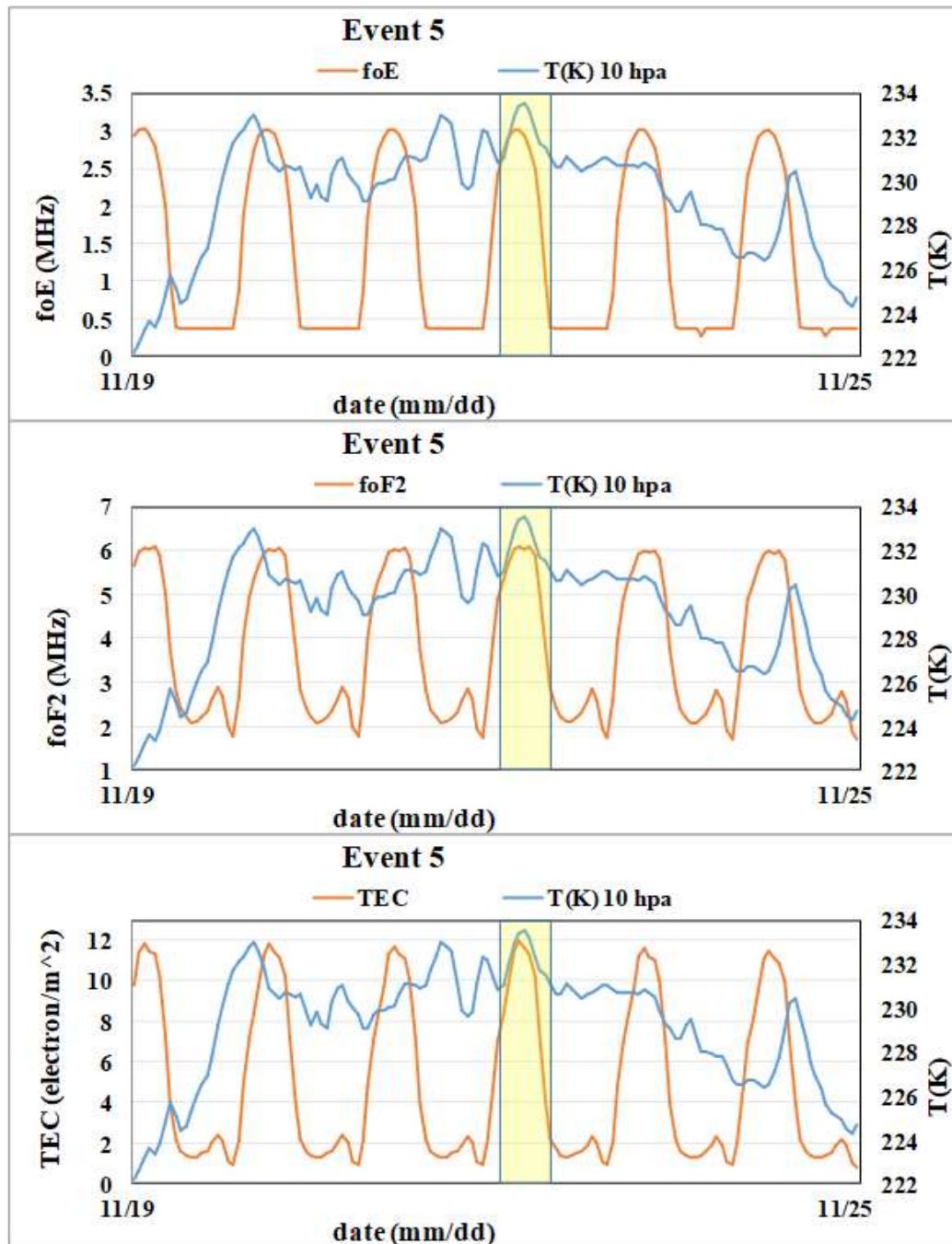


Figure 10: Ionospheric parameters with stratosphere temperature for event 5 year 2019

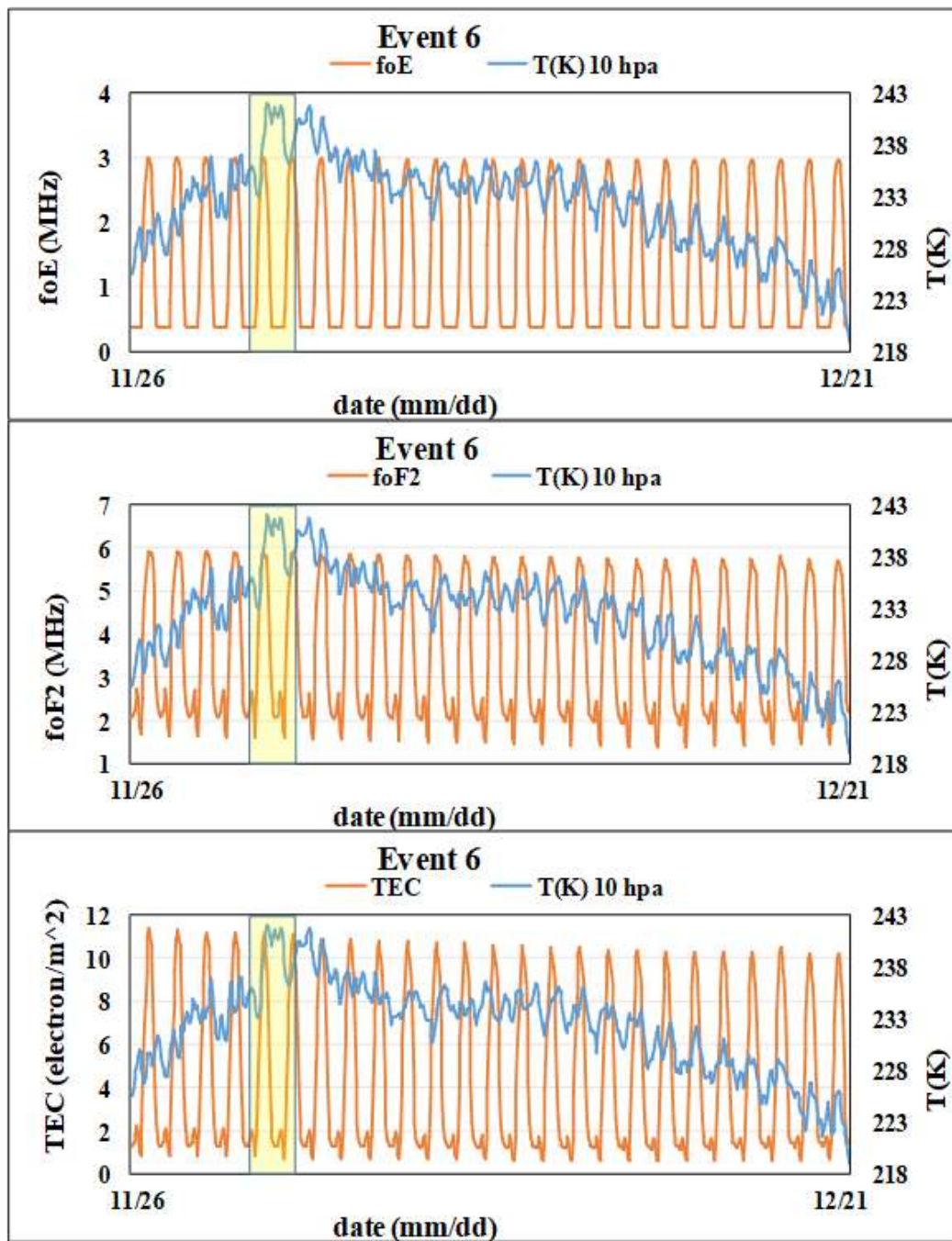


Figure 11: Ionospheric parameters with stratosphere temperature for event 6 year 2019.

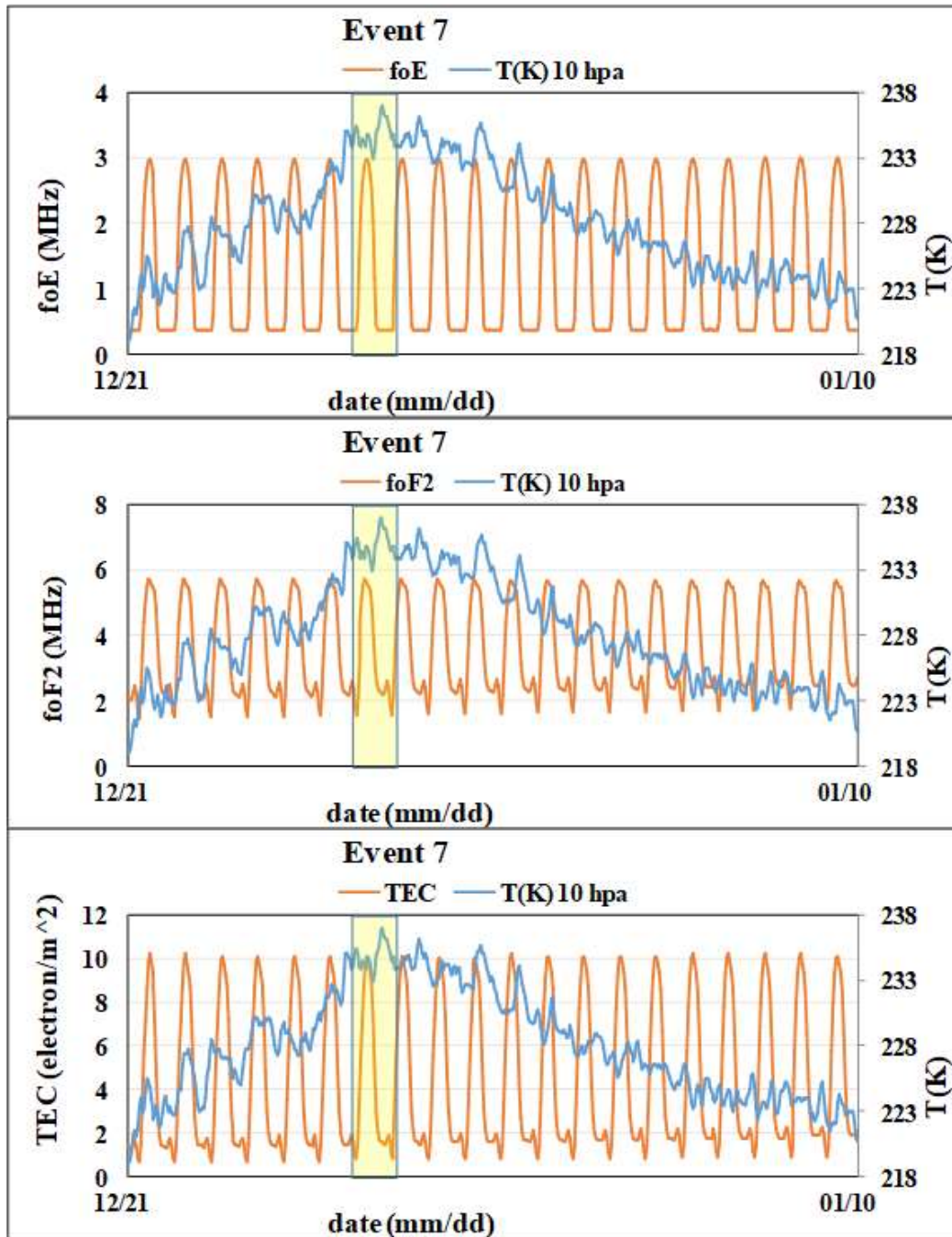


Figure 12: Ionospheric parameters with stratosphere temperature for event 7 year 2019.

3. Results and Discussion

Table 1 represented the events starting date (dd/mm/hh) with its temperature for each day, the maximum temperature value T_{Max} (K) with its variation from starting value ΔT (K), end date (dd/mm/hh) with its temperature, duration time in hours finally the percentage of increasing temperature between starting and maximum temperature. So from Fig. 5 and Table 1 it found that in 2014 the two events (1 and 2) lasted from the 3rd to the 17th of January and event (3) started from 8 to 14 February 2014, while in 2019 the event (4) lasted 2-8 January, event (5) from 19 to 25 November, event (6) from 26 November to 21 December and event (7) from 21 December 2019 to 10 January 2020 it reveals that all seven events are occurred in winter time. The longest period the

SSW lasted for 601 hours approximately 25 days or three and half weeks was in 2019 the event (6), while the shortest period for SSW was in 2014 the event (2) lasted 106 hours or four days less than week. It is clear from this that each event varies from one to another according to the circumstances, but it can be said that they all occurred during the winter time.

To understand the effect of SSW events on the ionosphere for Basrah city, so the IRI model with version 2020 which is developed to geomagnetic storms for all geographic latitudes is used to get the data for three ionospheric parameters, the critical frequency foE and foF2 in MHz for two layers E and F2 and the total electron content (TEC $\times 10^{16}$ in electrons/m²). Each ionospheric parameter was plotted with the stratospheric temperatures for the seven SSW events, as shown in Figs 6-12, from these figures we can see that there are a clear impact of this warming on the ionosphere parameter TEC (at height 500km), it was found that there is a positive enhancement in the ionization in this region of the atmosphere due to the rise in the temperature of the stratosphere, and the increase continues for several days. According to other parameters foE (at height 100km) and foF2 (at height 300km) there are a small enhancement in critical frequency as well as the electron density according to equation (1) or enhancements in ionization.

In this research study, the ionospheric plasma density (or critical frequency and TEC) responses investigate in the case where the sudden stratospheric warming exists, In this research study, the ionospheric plasma density (or critical frequency and TEC) responses investigate for two years 2014 and 2019 where the sudden stratospheric warming (this warming is intra-atmospheric origin) exists, in these two years taken the solar activity represented by geomagnetic storms low Dst index (quite condition) and low solar radiation flux index (F_{10.7}) which carries the solar wind plasma (protons and electrons) to the ionosphere regions are absent. The time taken of the ionization variations from the Sun and changing the dynamics of the atmospheric circulation composition caused by SSW is about some weeks, while the geomagnetic storm is an order of magnitude smaller spend almost few days. In this special case, at mid-latitude in the Northern Hemisphere ionospheric electron density response during SSW events is confirmed.

The TEC variation is present remarkable in all events with positive ionization enhancement during the daytime reaching maximum afternoon then be down after the Sun setting, this perturbation occurred due to change in the thermosphere composition, temperature, winds, and the F2 region dynamo or in some mechanical way of the E region dynamic. The event which characterized by atmospheric dynamical variation in the polar stratosphere, causing coupling vertically between different layers of Earth's atmosphere regions and this strong coupling impacts is play an important role in the ionospheric perturbations when the Sun is in its calm state (no solar activity).

4. Conclusions

Based on how well the above correlation works in the ionosphere's E and F2 regions, the E region's dynamics may play a big part in changing the mid-latitude ionosphere's electrodynamic. This variation is likely one of the main reasons for the TEC disturbance in the same region during the SSW events we've discussed. After looking at how TEC changed over two years in the middle latitude and talking briefly about the SSW event during those two years, the meridional wind in the mesosphere and lower thermosphere region helped make TEC stronger.

Acknowledgements

This work relates to University of Baghdad/ College of Science/ Department of Astronomy and Space. The authors would like to thank the cds.climate.copernicus.eu for providing the stratospheric hourly temperature data from ERA5 satellite, the WDC Kyoto Japan and geophysics data from UK WDC for solar SSN index, $F_{10.7}$ solar flux and Dst index data, also the IRI-20 prediction model which provide ionospheric parameters foE, foF2 and TEC, for whom I would like to introduce my utmost appreciation and thanks.

Conflict of Interest

Authors declare that they have no conflict of interest.

References

1. A. H. Butler, D. J. Seidel, S. C. Hardiman, N. Butchart, T. Birner, and A. Match, *Bull. Amer. Meteor. Soc.* **96**, 1913 (2015). DOI: 10.1175/BAMS-D-13-00173.1.
2. A. Mohammed and A.-U. N. Mr, *Int. J. Sci. Res.* **6**, 2319 (2017). DOI: 10.21275/ART20179007.
3. N. M. R. Al-Ubaidi and T. I. Zahra, *J. Geosci. Envir. Protect.* **6**, 12 (2018). DOI: 10.4236/gep.2018.62004.
4. L. P. Goncharenko, V. W. Hsu, C. G. M. Brum, S.-R. Zhang, and J. T. Fentzke, *J. Geophys. Res. Space Phys.* **118**, 472 (2013). DOI: 10.1029/2012JA018251.
5. J. Xu, K. Mohanakumar, D. Guo, Y. Liu, and J. Yue, *Adv. Met.* **2017**, 1 (2017). DOI: 10.1155/2017/3482462.
6. M. P. Baldwin and D. W. J. Thompson, *Quar. J. Roy. Met. Soci.* **135**, 1661 (2009). DOI: 10.1002/qj.479.
7. A. Y. Karpechko, F. Vitart, I. Statnaia, M. Alonso Balmaseda, A. J. Charlton-Perez, and I. Polichtchouk, *Quar. J. Roy. Met. Soci.* **150**, 1357 (2024). DOI: 10.1002/qj.4649.
8. J. L. Chau, L. P. Goncharenko, B. G. Fejer, and H.-L. Liu, *Space Sci. Rev.* **168**, 385 (2012). DOI: 10.1007/s11214-011-9797-5.
9. A. J. Charlton and L. M. Polvani, *J. Clim.* **20**, 449 (2007). DOI: 10.1175/JCLI3996.1.
10. G. Kakoti, B. R. Kalita, P. K. Bhuyan, S. Baruah, and K. Wang, *J. Geophys. Res. Space Phys.* **125**, e2020JA028570 (2020). DOI: 10.1029/2020JA028570.
11. S. R. Mawj and N. M. R. Al-Ubaidi, *IOP Conf. Ser. Earth Envir. Sci.* **1223**, 012009 (2023). DOI: 10.1088/1755-1315/1223/1/012009.
12. J. Laštovička, *J. Atmospher. Sol. Terrest. Phys.* **68**, 479 (2006). DOI: 10.1016/j.jastp.2005.01.018.
13. E. Yiğit and A. S. Medvedev, *Geosci. Lett.* **3**, 27 (2016). DOI: 10.1186/s40562-016-0056-1.
14. M. P. Baldwin, B. Ayarzagüena, T. Birner, N. Butchart, A. H. Butler, A. J. Charlton-Perez, D. I. V. Domeisen, C. I. Garfinkel, H. Garny, E. P. Gerber, M. I. Hegglin, U. Langematz, and N. M. Pedatella, *Rev. Geophys.* **59**, e2020RG000708 (2021). DOI: 10.1029/2020RG000708.
15. L. P. Goncharenko, V. L. Harvey, K. R. Greer, S. R. Zhang, and A. J. Coster, *J. Geophys. Res. Space Phys.* **125**, e2020JA028199 (2020). DOI: 10.1029/2020JA028199.
16. Z. Mošna, I. Edemskiy, J. Laštovička, M. Kozubek, P. Koucká Knížová, D. Kouba, and T. A. Siddiqui *Observation of the Ionosphere in Middle Latitudes During 2009, 2018 and 2018/2019 Sudden Stratospheric Warming Events.* *Atmosphere*, 2021. **12**, 602 DOI: |.
17. N. M. Pedatella and J. M. Forbes, *Geophys. Res. Lett.* **37**, L11104 (2010). DOI: <https://doi.org/10.1029/2010GL043560>.
18. N. M. Pedatella and H. L. Liu, *J. Geophys. Res. Space Phys.* **118**, 5333 (2013). DOI: 10.1002/jgra.50492.
19. N. M. Pedatella, H. L. Liu, F. Sassi, J. Lei, J. L. Chau, and X. Zhang, *J. Geophys. Res. Space Phys.* **119**, 3828 (2014). DOI: 10.1002/2014JA019849.
20. N. M. Pedatella, J. Oberheide, E. K. Sutton, H. L. Liu, J. L. Anderson, and K. Raeder, *J. Geophys. Res. Space Phys.* **121**, 3621 (2016). DOI: 10.1002/2016JA022528.
21. N. Pedatella, J. Chau, H. Schmidt, L. Goncharenko, C. Stolle, K. Hocke, V. Harvey, B. Funke, and T. Siddiqui, *Eos* **99**, 1 (2018). DOI: 10.1029/2018EO092441.
22. N. M. Pedatella and V. L. Harvey, *Geophys. Res. Lett.* **49**, e2022GL098877 (2022). DOI: 10.1029/2022GL098877.
23. N. M. Pedatella, *J. Geophys. Res. Space Phys.* **128**, e2023JA031495 (2023). DOI: 10.1029/2023JA031495.
24. Y. N. Korenkov, V. V. Klimenko, M. V. Klimenko, F. S. Bessarab, N. A. Korenkova, K. G. Ratovsky, M. A. Chernigovskaya, A. A. Shcherbakov, Y. Sahai, P. R. Fagundes, R. De Jesus, A. J. De Abreu, and P. Condor, *J. Geophys. Res.* **117**, A10309 (2012). DOI: 10.1029/2012JA018018.

25. O. F. Jonah, E. R. De Paula, E. A. Kherani, S. L. G. Dutra, and R. R. Paes, *J. Geophys. Res. Space Phys.* **119**, 4973 (2014). DOI: 10.1002/2013JA019491.
26. P. R. Fagundes, L. P. Goncharenko, A. J. De Abreu, K. Venkatesh, M. Pezzopane, R. De Jesus, M. Gende, A. J. Coster, and V. G. Pillat, *J. Geophys. Res. Space Phys.* **120**, 7889 (2015). DOI: 10.1002/2014JA020649.
27. E. Yiğit, P. Koucká Knížová, K. Georgieva, and W. Ward, *J. Atmosph. Sol. Terrest. Phys.* **141**, 1 (2016). DOI: 10.1016/j.jastp.2016.02.011.
28. F. Vieira, P. R. Fagundes, K. Venkatesh, L. P. Goncharenko, and V. G. Pillat, *J. Geophys. Res. Space Phys.* **122**, 2119 (2017). DOI: 10.1002/2016JA023650.
29. F. Vieira, P. R. Fagundes, V. G. Pillat, E. Agyei-Yeboah, K. Venkatesh, and M. O. Arcanjo, *J. Atmosph. Sol. Terrest. Phys.* **240**, 105945 (2022). DOI: 10.1016/j.jastp.2022.105945.
30. Y. Wang, V. Shulga, G. Milinevsky, A. Patoka, O. Evtushevsky, A. Klekociuk, W. Han, A. Grytsai, D. Shulga, V. Mysenko, and O. Antyufeyev, *Atmos. Chem. Phys.* **19**, 10303 (2019). DOI: 10.5194/acp-19-10303-2019.
31. G. Liu, W. Huang, H. Shen, E. Aa, M. Li, S. Liu, and B. Luo, *Space Weath.* **17**, 1230 (2019). DOI: 10.1029/2019SW002160.
32. Y. Shi, O. Evtushevsky, G. Milinevsky, X. Wang, A. Klekociuk, W. Han, A. Grytsai, Y. Wang, L. Wang, B. Novosyadlyj, and Y. Andrienko, *Atmosph. Res.* **297**, 107112 (2024). DOI: 10.1016/j.atmosres.2023.107112.
33. K. R. Greer, L. P. Goncharenko, V. L. Harvey, and N. Pedatella, *J. Geophys. Res. Space Phys.* **128**, e2023JA031797 (2023). DOI: 10.1029/2023JA031797.
34. J. Gogoi, K. Bhuyan, S. K. Sharma, B. R. Kalita, and R. Vaishnav, *Adv. Space Res.* **71**, 3357 (2023). DOI: 10.1016/j.asr.2022.12.003.
35. A. F. Abed, E. F. Khanjer, and S. A. Abdullah, *IOP Conf. Ser. Mater. Sci. Eng.* **757**, 012038 (2020). DOI: 10.1088/1757-899X/757/1/012038.
36. N. Al-Ansari, *J. Earth Sci. Geotech. Eng.* **11**, 1 (2021). DOI: 10.47260/jesge/1121.
37. A. a. A. Al-Shallal and N. M. R. Al-Ubaidi, *Iraqi J. Sci.* **61**, 3434 (2020). DOI: 10.24996/ij.s.2020.61.12.31.
38. D. Bilitza, M. Pezzopane, V. Truhlik, D. Altadill, B. W. Reinisch, and A. Pignalberi, *Rev. Geophys.* **60**, e2022RG000792 (2022). DOI: 10.1029/2022RG000792.
39. A. Pignalberi, D. Bilitza, P. Coisson, H. Haralambous, B. Nava, M. Pezzopane, F. Prol, A. Smirnov, D. R. Themens, and C. Xiong, *Adv. Space Res.* **In Press**, 1 (2024). DOI: 10.1016/j.asr.2024.05.056.
40. N. M. Al-Ubaidi, R. F. H. Foadi, and S. I. Gburi, *Iraqi J. Sci.* **65**, 6134 (2024). DOI: 10.24996/ij.s.2024.65.10(SI).20.
41. R. Bojilova and P. Mukhtarov, *Universe* **9**, 351 (2023). DOI: 10.3390/universe9080351.
42. D. Bilitza and C. Xiong, *Adv. Space Res.* **68**, 2124 (2021). DOI: 10.1016/j.asr.2020.11.012.
43. N. Servan-Schreiber, M. Aggarwal, Y. Huang, M. Kang, A. Shaker, and D. Bilitza, *Adv. Space Res.*, (2024). DOI: 10.1016/j.asr.2024.07.009.
44. P. A. Fontes, M. T. a. H. Muella, L. C. A. Resende, R. De Jesus, P. R. Fagundes, P. P. Batista, V. G. Pillat, A. Tardelli, and V. F. Andrioli, *J. Atmosph. Sol. Terrest. Phys.* **256**, 106199 (2024). DOI: 10.1016/j.jastp.2024.106199.

دراسة تأثير الاحترار المفاجئ في الستراتوسفير على الايونوسفير فوق مدينة البصرة

حوراء حازم¹ ونجاة محمد رشيد رؤوف¹

¹قسم الفلك والفضاء، كلية العلوم، جامعة بغداد، بغداد، العراق

الخلاصة

تعتبر ظاهرة الاحتباس الحراري المفاجئ في طبقة الستراتوسفير (SSW) خلال فصل الشتاء من الأمور المهمة التي تؤثر على الاتصالات عبر منطقة الأيونوسفير. وفي هذا البحث تم دراسة تأثير ارتفاع درجة حرارة الستراتوسفير المفاجئ عبر ذروة درجة الحرارة على ثلاثة معلمات أيونوسفيرية وهي التردد الحرج foE و foF2 للطبقتين E و F2 على التوالي والمحتوى الإلكتروني الكلي (TEC) باستخدام نموذج IRI-20 فوق مدينة البصرة (30.4 درجة شمالاً؛ 47.7 درجة شرقاً) الواقعة في جنوب العراق وتغطي منطقة خطوط العرض المتوسطة الجغرافية. تم أخذ عامين لهذه الدراسة 2014 (الحد الأقصى للبقع الشمسية SSN) و 2019 (الحد الأدنى للبقع الشمسية SSN) من الدورة الشمسية 2024. تم أخذ ارتفاع ضغطي 10hpa (~30 كم) لدرجة حرارة الستراتوسفير لكل ساعة ولنفس السنوات، ووجد أن هناك (7) أحداث SSW خلال هذه الفترة، ثلاثة منها في عام 2014 وأربعة الأخرى في عام 2019. تمت دراسة العلاقة بين درجات حرارة الستراتوسفير والمعلمت الأيونوسفيرية لإيجاد هذا التأثير، كشفت النتائج عن وجود علاقات غير خطية بينهما خلال جميع ساعات الأحداث ولكن هناك زيادة في التأين أثناء الأحداث. التباين في قيم TEC موجود بشكل ملحوظ في جميع الأحداث مع تعزيز التأين الإيجابي أثناء النهار ليصل إلى أقصى حد بعد الظهر ثم ينخفض بعد غروب الشمس، بينما يكشف foE و foF2 عن اضطراب طفيف حدث بسبب التغيير في تركيبة الغلاف الحراري ودرجة الحرارة والرياح ودينامو المنطقة F2، أو بطريقة ما دينامو المنطقة E والتي تؤثر أيضاً على تعزيز قيم TEC. هذه الزيادة في قيم معاملات الأيونوسفير غير منتظمة مع الوقت وتختلف من معامل إلى آخر.

الكلمات المفتاحية: مدينة البصرة، التردد الحرج، الأيونوسفير، الاحترار المفاجئ في الستراتوسفير، المحتوى الإلكتروني الكلي.